STRUCTURE AND MIXING OF A SWIRLING TRANSVERSE JET INTO A CROSSFLOW

Jordan A. Denev, Jochen Fröhlich, Henning Bockhorn
Institute for Technical Chemistry und Polymer Chemistry
University of Karlsruhe
Kaiserstrasse 12, 76128 Karlsruhe, Germany
{denev,froehlich,bockhorn}@ict.uni-karlsruhe.de

ABSTRACT

Large Eddy Simulation is used to investigate the flow field of a turbulent jet emerging into a laminar crossflow. In the jet, swirl is introduced by means of body forces with swirl number up to $S = 0.6$ in the pipe. The impact of the jet swirl on the flow field and in particular on the mixing is investigated by means of various analyses. It turns out that the resulting flow and concentration fields are substantially distorted by the swirl but the overall mixing as determined by cross-sectional spatial and temporal mixing indices is only little influenced.

INTRODUCTION

Mixing is one of the central issues in fluid mechanics and process engineering and relevant for a wide range of applications. These can involve the mixing of different fluids, mixing of fluids with different temperatures or different turbulence characteristics, etc. A configuration often employed for this purpose is that of a jet into a crossflow (JICF) which is used in many devices of process engineering or installations of chemical technology. Prominent examples are provided by gas turbine burners or chimneys. In the average flow, a JICF features a counter–rotating vortex pair (CVP) due to the entrainment of the jet along its sides by the crossflow. This motion transports crossflow fluid into the core of the jet so that the mixing rate of a JICF is higher than the one of a straight jet (Broadwell and Breidenthal, 1984). It is now of interest to investigate whether the mixing rate can be enhanced further by additional modifications applied to the configuration. In combustion and air conditioning, for example, straight swirling jets are frequently employed so that the question arises if additional swirl of the jet would enhance its mixing with the crossflow. This question is addressed in the present paper.

While the literature about the JICF is abundant (Margason, 1993) investigations concerned with the effect of initial swirl of the jet are extremely scarce. The only publications the present authors became aware of in the course of this research are Kavasaoğlu and Schetz (1989) and Yağci and Kavasaoğlu (1993), the first reporting on measurements of surface pressure and mean flow in the centerplane for low and medium swirl while the second presents computations for the same cases employing a statistical turbulence model. In the experiments, however, the crossflow at low Reynolds number was forced to be turbulent by means of roughness elements. The corresponding simulations were tuned to match this situation and only coarse-grained data on the average flow are presented.

Against this background the present paper provides a detailed study of the effects of jet swirl on the flow field and the resulting mixing of jet fluid with the crossflow. This is performed by means of Large Eddy Simulation (LES).

PHYSICAL AND NUMERICAL MODEL

The JICF, although geometrically simple at first sight, is a flow of substantial complexity. Different vortex systems coexist and interact, determining the properties of the flow to a substantial extent (Fric and Roshko, 1994). For this reason, Large Eddy Simulation (LES) is a suitable approach for its computation (Jones and Wille, 1996; Yuan *et al.*, 1999; Wegner

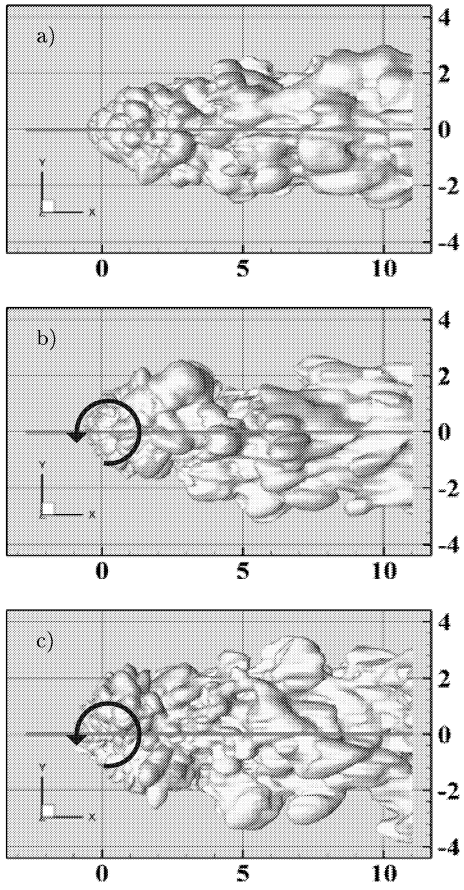

Figure 1: Instantaneous iso–concentration surfaces with $S_1 = 0.1$ viewed from top. a) $S = 0$, c) $S = 0.4$, c) $S = 0.6$.

Table 1: Overwiew over the simulations performed: swirl number at $z = -D$, averaging time, average time step and height of the trajectory at $x = 6D$.

case	S	t_{aver}	$\langle \Delta_t \rangle$	$z_{traj}(x = 6D)$
S00	0	101.8	0.00099	4.95
S02	0.2	102.1	0.00106	4.43
S04	0.4	100.4	0.00071	4.06
S06	0.6	102.2	0.00047	2.87

et al., 2004) while statistical models encounter difficulties with this type of flow (Demuren, 1993). In earlier work, (Fröhlich *et al.*, 2004), the present authors performed LES of a non-swirling jet into a crossflow and validated their approach by simulations similar to the ones of Yuan *et al.* (1999). The Smagorinsky model turned out to be sufficient for subgrid–scale modelling and is preferred here for robustness.

The principal computational domain extends over $x = -2.7D \dots 11D$, $y = -4D \dots 4D$, $z = -D \dots 12D$ in streamwise, spanwise and wall normal direction, respectively, where D is the diameter of the jet. The bottom wall is located at $z = 0$ and the outlet of the jet is centered at the origin of the coordinate system. At $z = -D$, turbulent inflow conditions were prescribed generated by a precursor simulation of turbulent swirling pipe flow with periodic boundary conditions in axial direction (García-Villalba *et al.*, 2004) and a period length of $5D$. The required mass flux was imposed by instantaneously adjusting an axial volume force, constant in space, to yield the desired flow rate $\dot{m}_{jet} = U_{jet}\rho\pi D^2/4$. Additionally, swirl was imposed by a corresponding volume force in tangential direction so as to generate the desired value of the swirl number

$$S = \frac{\int_0^{D/2} \rho\, u_a\, u_t\, r^2\, dr}{D/2 \int_0^{D/2} \rho\, u_a^2\, r\, dr}\,, \qquad (1)$$

where u_a and u_t are the axial and tangential velocity component, respectively. The inflow boundary condition for the crossflow was laminar with constant velocity U_∞ apart from a Blasius boundary layer of thickness equal to $D/2$ near the wall. Symmetry conditions were applied at the sides and a convective condition at the outlet.

The block–structured curvilinear Finite–Volume LES code LESOCC2 (Hinterberger, 2004) was used to solve the filtered equations. All computations were performed with the same numerical grid comprising about 1.5 Mio cells in 45 blocks. Typical cell sizes are $\Delta_z = 0.06D$ near the bottom wall as well as within the pipe and $\Delta_r = 0.009D$ in radial direction near the pipe wall. This results in $\Delta_r^+ = 4$ and $\Delta_z^+ = 26$ in the pipe and $\Delta_z^+ = 5$ near the inflow boundary condition (Fröhlich *et al.*, 2004). Along solid walls a wall function was employed the influence of which is little due to the relatively fine grid. The Smagorinsky model with $C_s = 0.1$ was used for sub-grid scale modelling in the momentum equation. An equation for a passive scalar with concentration S_1 is solved as well with boundary condition $S_1 = S_{1,jet} = 1$ in the pipe, $S_1 = 0$ in the crossflow, a convective outlet condition and homogeneous Neumann conditions at the remaining boundaries. Sub-grid scale mixing is represented by a turbulent diffusivity with turbulent Schmidt number of 0.6. In all computations, the Reynolds number based on the crossflow velocity and the jet diameter was $Re = 2100$ and the velocity ratio was $R = U_{jet}/U_\infty = 3.3$.

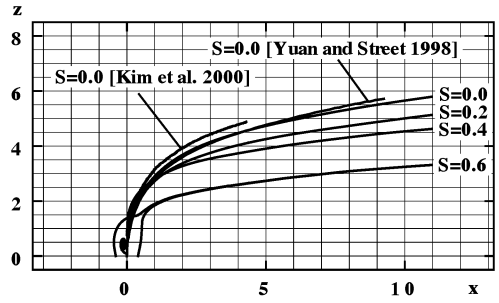

Figure 2: Trajectory of the JICF for different swirl numbers. For $S = 0,\ 0.2,\ 0.4$ the streamline of the average flow going through the origin of the coordinate system is plotted. For $S = 0.6$, this streamline remains close to the outlet so that the two lines through $x = \pm 0.4, y = 0, z = 0$ are shown in addition.

VALIDATION

The method applied corresponds to the one in (Fröhlich *et al.*, 2004) where a jet in crossflow was computed under the same conditions as in the present work but without swirl. This simulation is introduced in Table 1 as Case S00 and has been validated in the cited reference against LES by Yuan and Street (1998) and Yuan *et al.* (1999) as well as experiments from Sherif and Pletcher (1989) and good agreement was found. Recently, the authors also learned about PIV measurements for this non-swirling case by Kim *et al.* (2000), and these data are also introduced in Fig. 2.

Apart from the limited data with different crossflow conditions (Kavasaoğlu and Schetz, 1989; Yağci and Kavasaoğlu, 1993) mentioned above, no data were available up to now for a swirling jet into a crossflow.

OVERVIEW OVER COMPUTATIONS PERFORMED

In the present paper, the amount of jet swirl is characterized by the value of S imposed at $z = -D$. Table 1 provides an overview over the simulations discussed below. All simulations were carried out for at least 22 time units D/U_∞ before starting the collection of statistics. Then, averaging was performed for more than 100 time units as indicated in the table. The time step was adaptively adjusted to yield a maximum CFL number of 0.6 during the run which resulted in smaller time steps with increasing swirl as reflected by the average size of the time step as reported in Table 1 .

INSTANTANEOUS FLOW FIELD

Fig. 1 provides a first impression of the flow by means of top views of the instantaneous iso-concentration surface $S_1 = 0.1$ for $S = 0,\ 0.4$, and 0.6. It can be observed in these pictures that the overall character of the flow is not drastically changed with $S = 0.4$ but that the surface becomes rougher with $S = 0.6$. Also, further downstream large pockets of crossflow fluid tend to enter the jet to a higher degree than in the other cases. The straight line introduced in these pictures shows that the amount of asymmetry in y–direction is only small. It

appears to be somewhat stronger for $S = 0.4$ than for $S = 0.6$. Asymmetry of the flow field is better assessed by means of the average flow field discussed below.

The jagged structure of the concentration iso-surfaces reflects the large-scale mixing of the jet with the crossflow. The plots show that there is no immediate qualitative difference in the mixing process between jet and crossflow when swirl is added to the jet. It appears, however, that the structures near the jet's outlet are somewhat finer with $S = 0.6$. A higher degree of mixing indeed is observed in the analysis below.

AVERAGE FLOW

Side views of instantaneous data and averages reveal that with increasing swirl the jet intrudes substantially less into the crossflow. Fig. 2 shows the trajectory of the jet, defined as the average streamline through the center of the outlet, together with data from the literature for the non-swirling case. For $S = 0.6$, a recirculation region occurs in the center of the jet so that the corresponding streamline remains in this area, resulting in a small dot near the origin in this figure. Hence, the two average streamlines through the points $(\pm 0.4, 0, 0)$ were used to visualize the position of the jet in this case. The height of the jet is quantified by the position of the trajectory at $x = 6D$ and given in Table 1. The corresponding value in (Yuan *et al.*, 1999) is 5.02. Hence, very good agreement for the trajectory of the jet is found between the LES of this paper and the present data. Both are somewhat lower but still close to the experimental data of Kim *et al.* (2000).

The occurence of a recirculation region near the outlet is in agreement with the literature on swirling jets into quiescent flow. Beér and Chigier (1972), e.g., distinguish between low-swirl cases with $S < 0.6$ exhibiting no recirculation zone and high-swirl cases $S > 0.6$ with recirculation close to the outlet, although the data reproduced in this reference already exhibit a pronounced recirculation region for $S = 0.6$. The present simulations hence demonstrate that, when issued into a crossflow, the behaviour immediately at the outlet is simmilar to the pure swirling jet. It will be shown in the sequel that swirl with $S = 0.6$ substantially changes the behaviour of the entire jet.

Fig. 3 provides quantitative data on the velocity magnitude and its fluctuations. These are defined as

$$U_m = \sqrt{u^2 + v^2 + w^2}; \quad U_{rms} = \sqrt{\langle (U_m - \langle U_m \rangle)^2 \rangle} \qquad (2)$$

in order to allow for comparison with hot wire data which are insensitive to the direction of the flow (throughout, $\langle \ldots \rangle$ denotes time averaging and a prime the corresponding fluctuations). With S increasing up to 0.4, the profile of U_m at the outlet $x/D = 0$ becomes broader and the upper maximum at $x = 1.83D$ is reduced substantially while the lower one approaches the bottom wall. The fluctuations show a change towards a broader and somewhat lower upper peak while the near-wall behaviour appears to be little influenced.

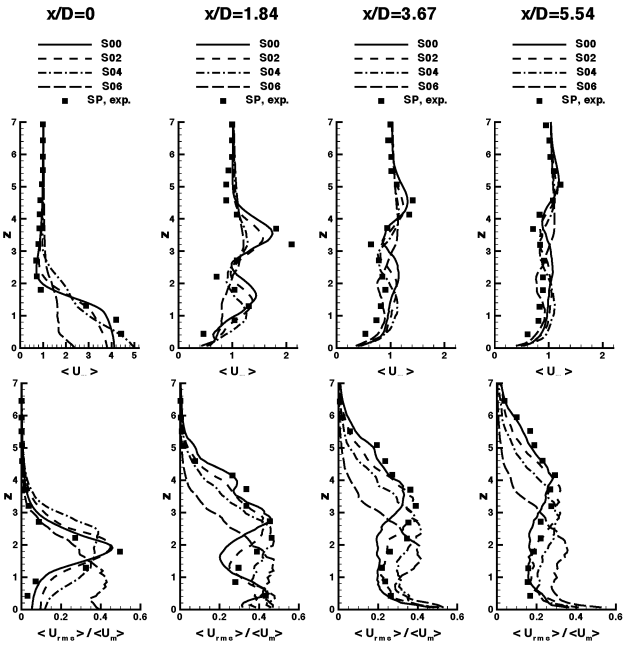

Figure 3: Profiles of mean velocity magnitude and fluctuations along vertical lines in the centerplane $y = 0$ at different streamwise positions. The symbols represent the data of Sherif and Pletcher (1989) for $S = 0$. Upper row: mean velocity magnitude U_m, lower row: rms-fluctuations of the velocity magnitude.

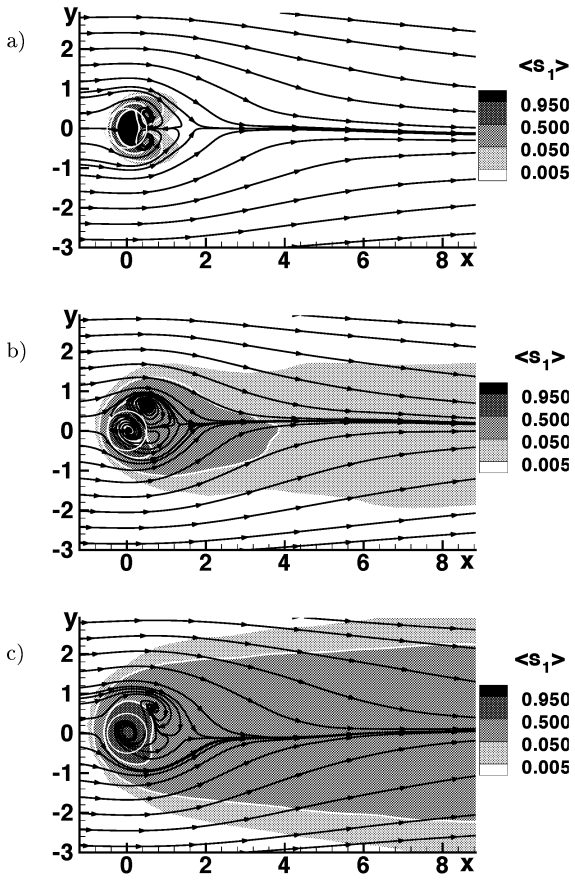

Figure 4: Average streamlines and concentration in the wall-parallel plane $z = 0.5D$. a) $S = 0$, c) $S = 0.4$, c) $S = 0.6$. the jet outlet is marked by a white circle.

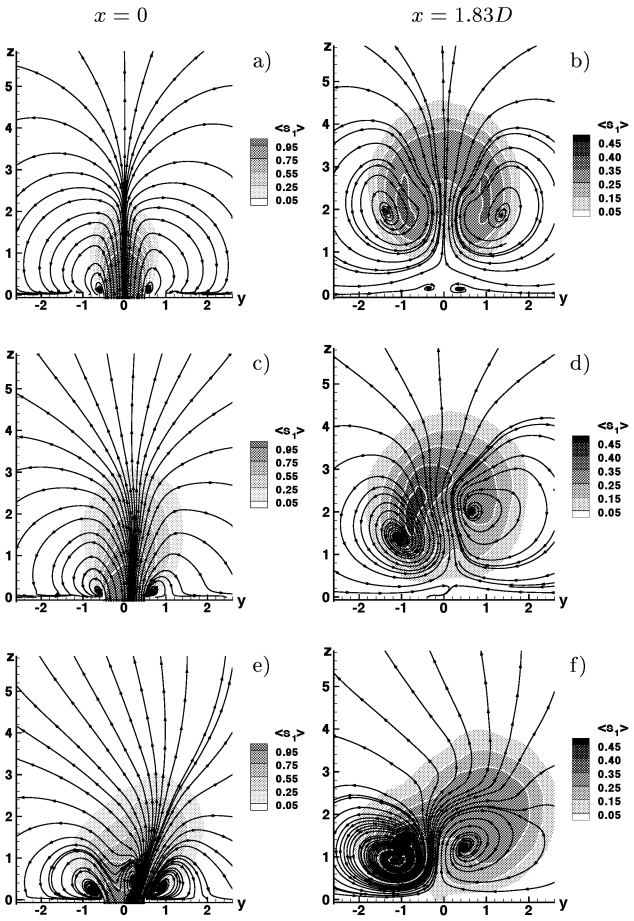

Figure 5: Average streamlines and concentration in planes $x = 0$ (left) and $x = 1.83$ (right). a,b) $S = 0$, c,d) $S = 0.4$, e,f) $S = 0.6$.

For $S = 0.6$, in contrast, the recirculation zone results in small values of velocity at the center of the outlet and a substantially flatter U_m-profile. The peak of the fluctuations also appears much closer to the wall, resulting from the lower trajectory (Fig. 2), and for the downstream positions somewhat stronger than in the other cases.

Fig. 4 presents average streamlines and average concentration of the scalar introduced with the jet, $\langle S_1 \rangle$, in the plane $z = 0.5D$ for $S = 0, 0.4$, and 0.6. The streamlines reveal that the jet swirl yields a distorted, asymmetric vortex pattern at the outlet of the jet with the hanging vortex suppressed for $y < 0$ and enhanced for $y > 0$. This is caused by increased lateral shear between the jet fluid and the crossflow on one side and a corresponding reduction of the shear on the opposite side. The concentration exhibits asymmetry for $S = 0.4$ while apearing quite symmetrical for $S = 0.6$. Its overall level increases with swirl since the jet trajectory more and more approaches the wall. This is visible in Fig. 5 assembling plots analogeous to the previous ones in cross sections at $x = 0$ and $x = 1.83D$. The latter shows the CVP in the average flow resulting from the shear between jet and crossflow. The difference between the data for $S = 0$ and $S = 0.4$ is relatively small; the flow field becomes asymmetric with the left vortex of the CVP being stronger, as also revealed by plots of the average vorticity in $x-$direction (not shown here). The induced vortex pair at the wall is still present but reduced in strength. The asymmetry of the flow field is accompanied by a shift of the concentration maximum to $y < 0$. For $S = 0.6$ in contrast, the streamlines are substantially inclined at the outlet and the inner recirculation is also visible. Further downstream, the asymmetry in the flow and concentration field is quite pronounced. It is well known that without swirl the centers of the CVP and the maxima of concentration do not coincide close to the outlet. With swirl, the relative position changes from the centers being at the same wall distance but outward of the concentration maximum (Fig. 5b) to being below it (Fig. 5f). Further information in this respect is given in Fig. 7 below. Further downstream, for $x = 3 \ldots 8$, the stronger vortex and the concentration maximum, coincide for $S = 0.6$.

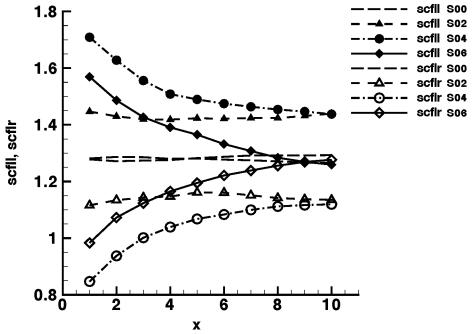

Figure 6: Average scalar flux through right and left half of the computational domain for different amounts of swirl. Open symbols: $y > 0$, closed symbols: $y < 0$.

Quantification of scalar mixing

The amount of asymmetry in the flow field impacts on the mixing between jet and crossflow. Each cross section $x = const.$ hence was split into the left sector with $y > 0$ and and the right sector with $y < 0$, and all quantities were determined for the sectors independently. This was performed by interpolating on a two-dimensional cartesian grid.

An interesting quantity in this respect is the scalar flux $\langle u_x S_1 \rangle = \langle u_x \rangle \langle S_1 \rangle + \langle u'_x S'_1 \rangle$ depicted in Fig. 6. At steady state, its total value is $U_{jet} \pi D^2/4 \, S_{1,jet} = 2.59$ for conservation reasons. With increasing swirl the asymmetry of this quantity increases. It reduces with axial distance but curiously the fluxes settle to the same values, 1.45 and 1.15 for both, $S = 0.2$ and $S = 0.4$. With $S = 0.6$, in contrast, the asymmetry is reduced substantially faster in streamwise direction and vanishes already at $x = 9$.

Fig. 7 provides further information in this respect. Fig. 7a reveals that the average concentration is shifted towards $y < 0$ for small values of swirl, while for $S = 0.6$ it is larger on the opposite side. This reflects the increased region of jet fluid visible in Fig. 5f, while the maximum of scalar concentration is observed at $y < 0$. Fig. 7b shows the maximum value of concentration attained in both sectors and the corresponding asymmetry. The wall distance of their position is reported in Fig. 7c and the lateral position in Fig. 7d. Again, the behaviour for $S = 0.6$ is different from the other cases.

The wall distance of the maxima, e.g., is substantially lower. Comparison of Fig. 6 and Fig. 7a shows that the scalar transport is the result of a complex interaction between the local concentration and the flow field transporting the quantity.

Mixing is often assessed by means of so-called mixing indices. The most widely applied ones are the spatial mixing defficiency (SMD) and the temporal mixing deficiency (TMD). They are defined as

$$SMD = \frac{RMS(\langle S_1 \rangle - AVG(\langle S_1 \rangle))}{AVG(\langle S_1 \rangle)} \times 100\% \tag{3}$$

$$TMD = AVG\left(\frac{\sqrt{\langle S_1' S_1' \rangle}}{\langle S_1 \rangle}\right) \times 100\%. \tag{4}$$

Here, AVG denotes spatial averaging and RMS the root-mean-square in the spatial sense. The quality of mixing increases with lower values of the indices. A difficulty with the TMD is the appearance of the average $\langle S_1 \rangle$ in the denominator. Its value tends to zero in the boundaries of the jet and the outer flow resulting in a singularity of the index. For this reason, only points with $\langle S_1 \rangle > 0.01$ $S_{1,jet} = 0.01$ were taken into account when evaluating this quantity. Tests by Denev *et al.* (2005) revealed that this restriction only changes the level but not the decay of the TMD with x when applied to a JICF without swirl. The SMD, in contrast can be evaluated without any restriction since the denominator is first averaged in space before division.

Fig. 8 and 9 show the values of SMD and TMD computed with the present data. With increasing swirl, the SMD decreases, indicating better mixing, but at $x = 10$ the difference between the cases is relatively small. It is reduced from 131% with $S = 0$ to 125% with $S = 0.6$. Observe, however the larger range of the abscissa compared to Fig. 9. The TMD first increases with increasing swirl indicating higher average intermittency of scalar concentration. For $S = 0.6$, again, the behaviour is different since the TMD is lower than with $S = 0.4$ and decreases faster than in the other cases. At $x = 10$ it has about the same value for $S = 0.6$ than without swirl while being larger closer to the outlet.

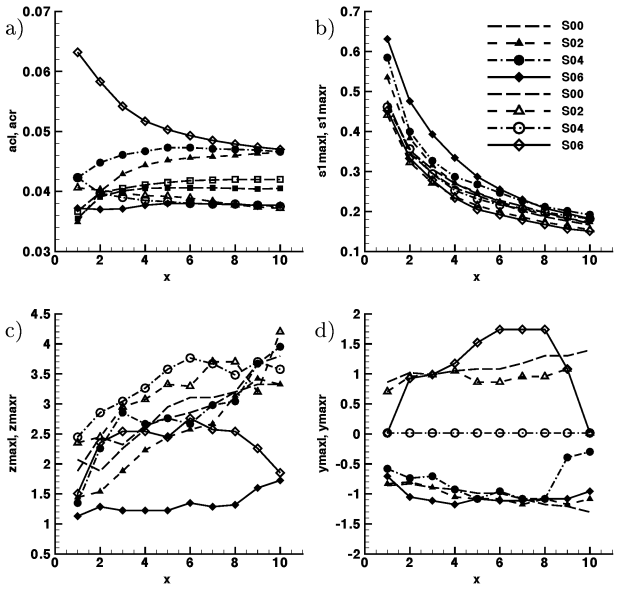

Figure 7: Asymmetry of the mean flow field for different swirl numbers with legend according to the upper right picture. Quantities have been determined in cross sections $x = const.$ and sector $y > 0$ (open symbols) and $y < 0$ (closed symbols). a) average scalar concentration in left and right half of the cross-sectional plane, with integration up to $z = 8$ only, for technical reasons, b) maximum of scalar concentration, c) distance from the wall of the point where the maximum is attained, d) spanwise position of the maximum.

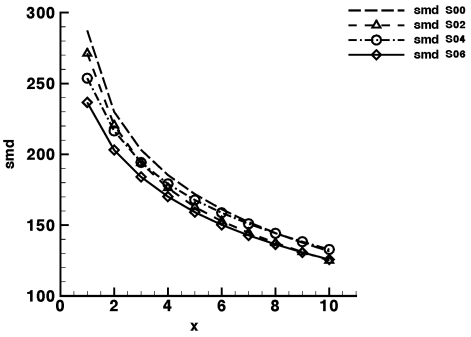

Figure 8: Spatial mixing index SMD in cross sections $x = const.$ for different swirl numbers.

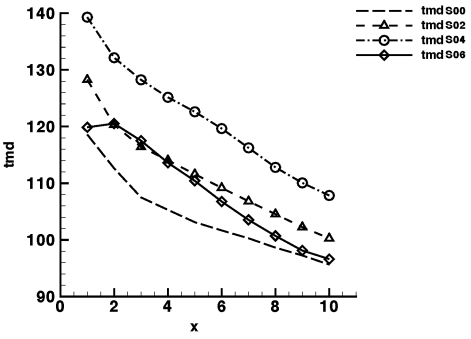

Figure 9: Temporal mixing index TMD in cross sections $x = const.$ for different swirl numbers. The computation is restricted to the area where $\langle S_1 \rangle > 0.01$.

Conclusions

Large eddy simulations of a jet into a crossflow were performed with different amounts of additional swirl in the pipe flow. Comparison of results for the non-swirling case with data from the literature shows good agreement and validates the approach.

Responding to the initial question, of whether additional swirl would increase the mixing of a JICF, the present results show that this is not or at least not substantially observed. This conclusion addresses the overall amount of mixing. It is supported by quantification of mixing utilizing the spatial and the temporal mixing deficiency in cross sectional planes $x = const.$ While the SMD index shows a small improvement for the cases with swirl, the TMD index displays poorer mixing, for the cases with low swirl ($S = 0.2$ and $S = 0.4$).

The cases with strong swirl exhibits a substantial modification of the flow patterns, starting from a recirculation region on the jet axis at the outlet of the pipe. This modification considerably influences the complete behaviour of the JICF as addressed by consideration of diverse quantities reported in the paper. This is in particular the case for the scalar flux through the left ($y < 0$) and right ($y > 0$) sector. While these remain asymmetric with $S = 0.2$ and $S = 0.4$, they return to symmetry in the case $S = 0.6$ within a distance of $x/D = 9$ from the outlet.

Data from the present results will be available under `http://www.ict.uni-karlsruhe.de/index.pl/themen/dns/index.html`

Acknowledgments: The authors acknowledge funding by the German Research Foundation through the Priority Programme SPP-1141 "Analysis, Modelling and Computation of Mixing Devices with and without Chemical Reactions" and SFB 606 "Unsteady Combustion". M. García-Villalba kindly provided the routine for the generation of swirl in the inflow vane.

REFERENCES

Beér, J. and Chigier, N. (1972). *Combustion Aerodynamics*. Applied Science Publishers Ltd.

Broadwell, J. and Breidenthal, R. (1984). Structure and mixing of a transverse jet in incompressible flow. *J. Fluid Mech.*, **148**, 405–412.

Demuren, A. (1993). Characteristics of three–dimensional turbulent jets in crossflow. *Int. J. Engng Sci.*, **31**, 899–913.

Denev, J., Fröhlich, J., and Bockhorn, H. (2005). Evaluation of mixing and chemical reactions within a jet in crossflow by means of les. In *Proc. European Combustion Meeting, CD-ROM*. Université Catholique de Lauvain, Belgian Section of the Combustion Institute.

Fric, T. and Roshko, A. (1994). Vortical structure in the wake of a transverse jet. *J. Fluid Mech.*, **279**, 1–47.

Fröhlich, J., Denev, J., and Bockhorn, H. (2004). Large eddy simulation of a jet in crossflow. In *Proceedings of ECCOMAS 2004, Jyväskylä, Finland, July 24-28, ISBN 951-39-1868-8*, pages CD–ROM, Barcelona. CIMNE.

García-Villalba, M., Fröhlich, J., and Rodi, W. (2004). On inflow boundary conditions for large eddy simulation of turbulent swirling jets. In *XXI International Congress of Theoretical and Applied Mechanics 15 - 21 August 2004, Warsaw, Poland.*

Hinterberger, C. (2004). *Dreidimensionale und tiefengemittelte Large–Eddy–Simulation von Flachwasserströmungen.* Ph.D. thesis, Institute for Hydromechanics, University of Karlsruhe.

Jones, W. and Wille, M. (1996). Large-eddy simulation of a plane jet in a cross flow. *Int. J. Heat and Fluid Flow*, **17**, 296–306.

Kavasaoğlu, M. and Schetz, J. (1989). Effects of swirl and high turbulence on a jet in a crossflow. *J. Aircraft*, **26**(6), 539–546.

Kim, K., Kim, S., and Yoon, S. (2000). PIV measurements of the flow and turbulent characteristics of a round jet in crossflow. *J. Visualization*, **3**, 157–164.

Margason, R. (1993). 50 years of jet in cross flow research. *Computational and experimental assessment of jets in crossflow*, pages 1.1–1.41. AGARD-CP-534.

Sherif, S. and Pletcher, R. (1989). Measurements of the flow and turbulence characteristics of round jets in cross flow. *J. Fluids Eng*, **111**, 165.

Wegner, B., Huai, Y., and Sadiki, A. (2004). Comparative study of turbulent mixing in jet in cross-flow configurations using les. *submitted to Int. J. Heat Fluid Flow.*

Yağci, H. and Kavasaoğlu, M. (1993). Navier–Stokes analysis of a swirling jet in crossflow. In R. Margason, editor, *Computational and Experimental Assessment of Jets in Cross Flow*, volume CP-534, pages 38.1–38.7. AGARD.

Yuan, L. and Street, R. L. (1998). Trajectory and entrainment of a round jet in crossflow. *Phys. Fluids*, **10**(9), 2323–2335.

Yuan, L., Street, R., and Ferziger, J. (1999). Large–eddy simulations of a round jet in crossflow. *J. Fluid Mech.*, **379**, 71–104.